

**Conclusions:** For a moving target, it was confirmed that the 4D CBCT based registration provided more accuracy compared to 3D CBCT based registration.

#### PD-0044

##### Respiratory-induced motion of pancreatic cancer: time trends during the course of radiotherapy

E. Lens<sup>1</sup>, A. van der Horst<sup>1</sup>, G. van Tienhoven<sup>1</sup>, R. Dávila Fajardo<sup>1</sup>, P. Fockens<sup>2</sup>, J.E. van Hooft<sup>2</sup>, A. Bel<sup>1</sup>

<sup>1</sup>AMC Amsterdam, Radiotherapy, Amsterdam, The Netherlands

<sup>2</sup>AMC Amsterdam, Gastroenterology and Hepatology, Amsterdam, The Netherlands

**Purpose/Objective:** Irradiation of pancreatic tumors requires large margins to account for respiratory-induced intrafractional tumor motion. These margins are derived from a single pre-treatment 4DCT scan. This respiratory-induced intrafractional motion can be visualized using implanted fiducial markers.

The purpose of the current study is to quantify the respiratory-induced motion of pancreatic cancer, both on the 4DCT scan as well as on daily cone beam CT (CBCT) scans during a 5 week course of radiation to reveal possible trends during the course of treatment.

**Materials and Methods:** Eight patients (4 male / 4 female) with borderline resectable pancreatic cancer were treated with 25 x 2Gy plus weekly gemcitabine 300 mg/m<sup>2</sup>. All patients received 2 to 4 fiducial markers by endoscopic ultrasound-guided implantation. The amplitude of respiratory-induced motion was measured on the pre-treatment 4DCT scan and also on all available daily CBCT scans. Phase reconstructions of the CBCT scans were made by an automated selection of the 2D projection images corresponding to the peak inhale and exhale phases. These reconstructions were matched to the (reference) planning CT. The amplitudes (differences between the 2 extreme positions) were analyzed by matching on the markers (in three directions) and on the diaphragm (superior-inferior (SI) direction only). Rotations and deformations of the tissue were not analyzed. The amplitudes were linearly fit as a function of time (i.e. treatment day). The fits were tested for significance using a Student's t-test and statistical significance was assumed at p<0.05.

**Results:** The amplitude of intrafractional motion of the markers was greatest in the SI direction (mean 5.9mm, SD: 2.7mm on CBCT). Differences up to 5.1mm (range: 0.3 - 5.1 mm) were found between the amplitude on the 4DCT scan and the mean amplitude of all CBCT scans of a single patient.

The analysis of daily respiratory-induced motion of the markers revealed significant trends in the amplitude as a function of time (table and figure). The diaphragm did not always show the same trend as the markers. For the markers neither the amplitudes nor the trends were significant in the other 2 directions (data not shown).

**Conclusions:** The 4DCT used for treatment planning is often not representative of the respiratory-induced motion amplitude during treatment. The CBCT projection images showed significant time trends in the amplitude of respiratory-induced motion during a five week course of radiation. These time trends in the amplitudes indicate the usefulness of adaptive treatment procedures.

Patient #	# of available scans	Slope diaphragm mm/day	p-value	Slope markers mm/day	p-value
Patient 1	26	-0.054 ± 0.111	0.33	-0.011 ± 0.055	0.67
Patient 2	18	0.060 ± 0.106	0.25	0.097 ± 0.078	0.02
Patient 3	17	-0.102 ± 0.084	0.02	-0.009 ± 0.055	0.73
Patient 4	25	-0.134 ± 0.089	0.005	-0.030 ± 0.042	0.15
Patient 5	25	0.106 ± 0.073	0.007	-0.023 ± 0.037	0.20
Patient 6	25	-0.120 ± 0.051	<0.0001	-0.051 ± 0.046	0.03
Patient 7	26	0.051 ± 0.113	0.36	-0.083 ± 0.071	0.02
Patient 8	24	-0.084 ± 0.055	0.005	-0.038 ± 0.063	0.22

Table: Fit data of all patients in the SI direction for the amplitude of the diaphragm and the markers. The slopes are given in combination with the 95% confidence interval.

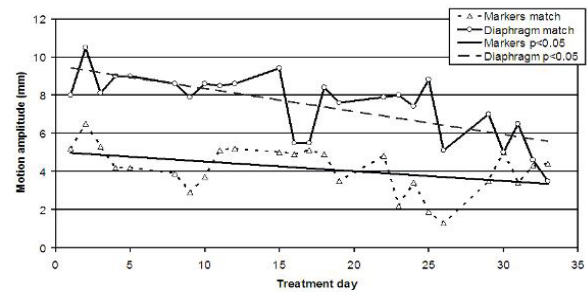


Figure: Amplitudes of respiratory-induced motion of the markers and diaphragm as a function of treatment day (i.e. time) for patient 6 (SI direction), where day 1 is measured using the CBCT made prior to the first fraction.

#### PD-0045

##### Time-resolved dose reconstruction of VMAT delivery to moving targets with and without dynamic MLC tracking

T. Ravkilde<sup>1</sup>, P.J. Keall<sup>2</sup>, C. Grau<sup>1</sup>, M. Hoyer<sup>1</sup>, P.R. Poulsen<sup>1</sup>

<sup>1</sup>Aarhus University Hospital, Department of Oncology, Aarhus, Denmark

<sup>2</sup>University of Sydney, Sydney Medical School, Sydney, Australia

**Purpose/Objective:** Dynamic multi-leaf collimator (DMLC) tracking can mitigate the dosimetric impact of target motion during volumetric modulated arc therapy (VMAT). However, residual dosimetric errors still exist. The purpose of this study was to create a simple model for time-resolved reconstruction of the delivered dose distribution and to validate its ability to predict the time-resolved dosimetric errors measured during VMAT of moving targets with and without DMLC tracking.

**Materials and Methods:** DMLC tracking experiments were performed on a Trilogy linear accelerator (Varian Medical Systems) connected to prototype DMLC tracking software. A three-axis motion stage, carrying a Delta4 phantom (Scandidos) on a custom built platform, reproduced eight representative tumor trajectories; four lung and four prostate. For each trajectory, two VMAT treatment plans (low and high modulation) were delivered with and without DMLC tracking. During tracking the MLC leaves were continuously refitted to the 3D target position measured by an electromagnetic RayPilot transponder (Micropos Medical) at 30 Hz. Doses were measured with the orthogonal detector arrays of the Delta4 phantom at a rate of 72 Hz. Offline, the measured doses were down-sampled to steps of 10 dose pulses to reduce noise (mean time resolution of 20 Hz). The time-resolved dose distribution was compared to a reference dose measured without target motion by use of time-resolved 3%/3mm  $\gamma$ -tests with exclusion of detectors receiving less than 5% of the maximum dose in the accumulated reference dose. For all experiments, the time-resolved dose delivered to each detector in the phantom was calculated by a simple model that included the target position, the MLC aperture convolved with a 2D dose kernel, the dose rate, and a percentage depth dose. Like for the measurements, the time-resolved 3%/3mm  $\gamma$ -test was also performed for the reconstructed doses by comparison with the reconstructed dose to a static phantom. Finally, the reconstructed and the measured  $\gamma$  failure rates were compared for each experiment.

##### Results:

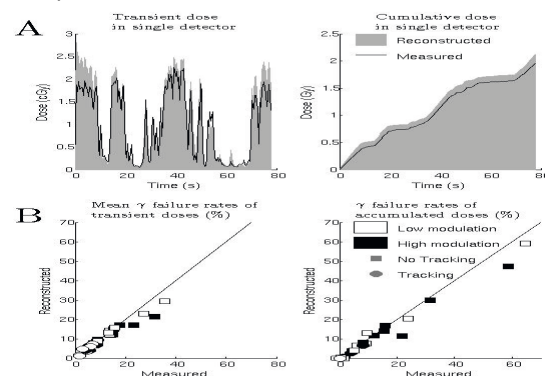


Fig. A compares the measured and reconstructed transient and cumulative doses for a single detector during beam delivery in one experiment. The scatter plots in Fig. B compare the measured and